

## Highly tensile-strained, type-II, Ga<sub>1-x</sub>In<sub>x</sub>As/GaSb quantum wells

T. Taliercio,<sup>1</sup> A. Gassenq,<sup>1</sup> E. Luna,<sup>2</sup> A. Trampert,<sup>2</sup> and E. Tournié<sup>1,a)</sup>

<sup>1</sup>Institut d'Electronique du Sud, UMR CNRS 5214, Université Montpellier 2, Place Eugène Bataillon, F-34095 Montpellier Cedex 5, France

<sup>2</sup>Paul-Drude Institute for Solid-State Electronics, Hausvogteiplatz 5-7, D-10117 Berlin, Germany

(Received 15 September 2009; accepted 11 January 2010; published online 9 February 2010)

We have investigated the properties of highly tensile-strained (Ga,In)As layers in a GaSb matrix. *In situ* observations of the growth mode suggest the formation of (Ga,In)As quantum dots. In contrast, *ex situ* transmission electron microscopy evidences the formation of perfect quantum wells with the presence of a (Ga,In)Sb interfacial layer. This is analyzed taking into account the surfactant behavior of Sb and stabilization of the system by reduction of the overall strain. Photoluminescence is observed up to 3.0  $\mu\text{m}$  at room temperature, in good agreement with calculations assuming a type-II band alignment and including the (Ga,In)Sb interfacial layer. © 2010 American Institute of Physics. [doi:10.1063/1.3303821]

Semiconductor nanostructures have been the subject of intense investigations for the past couple of decades driven by both fundamental as well as applied interests. Most work till now has focused on compressively strained systems such as Si<sub>1-x</sub>Ge<sub>x</sub> on Si or Ga<sub>1-x</sub>In<sub>x</sub>As on GaAs and it is now well documented that when the misfit strain is larger than  $\sim 2\%$ , the epitaxial growth under usual conditions proceeds according to the Stranski–Krastanov (SK) mode, i.e., by two-dimensional (2D) nucleation followed by a transition toward the formation of coherent three-dimensional (3D) islands.<sup>1</sup> This process is indeed used to generate self-organized quantum dots (QDs).<sup>2</sup>

The Ga<sub>1-x</sub>In<sub>x</sub>As alloy offers this peculiarity that its strain state can be adjusted from high compression (e.g.,  $\varepsilon = +7.2\%$  for InAs on GaAs) to high tension (e.g.,  $\varepsilon = -7.9\%$  for GaAs on GaSb), through zero or moderate compression or tension (e.g., Ga<sub>1-x</sub>In<sub>x</sub>As on InP), where the epitaxial strain is defined as  $\varepsilon = (a_{\text{layer}} - a_{\text{substrate}}) / a_{\text{layer}}$  and  $a_i$  is the lattice parameter of  $i$ . While the compressively strained cases have been studied at length,<sup>2</sup> the properties of tensile layers is less clear.

Tensile strained Ga<sub>1-x</sub>In<sub>x</sub>As/GaSb heterostructures exhibit several interesting features. The band alignment at the interface is type II with holes and electrons confined in GaSb and Ga<sub>1-x</sub>In<sub>x</sub>As, respectively.<sup>3</sup> In addition the tensile strain induces a strong reduction of the Ga<sub>1-x</sub>In<sub>x</sub>As band gap which may open the way to mid-IR applications for these heterostructures. In this work we have studied the properties of highly tensile-strained Ga<sub>1-x</sub>In<sub>x</sub>As alloys ( $0 \leq x \leq 0.50$ ) embedded in GaSb.

The samples were grown by solid-source molecular beam epitaxy (MBE) on (001)-GaSb substrates using a reactor equipped with arsenic and antimony valved cracker cells delivering As<sub>2</sub> and Sb<sub>2</sub> dimers. The optically active part of the samples consists in three to five repeats of the [30 nm GaSb/ $y$  monolayers (ML) Ga<sub>1-x</sub>In<sub>x</sub>As] sequence. The growth temperature of this sequence has been adjusted between 500 °C for GaAs and 420 °C for Ga<sub>0.50</sub>In<sub>0.50</sub>As to account for the increased In content. A 5 s growth interrup-

tion has been applied to the GaSb-to-Ga<sub>1-x</sub>In<sub>x</sub>As (lower) interfaces while no interruption has been applied to the Ga<sub>1-x</sub>In<sub>x</sub>As-to-GaSb (upper) interfaces. These active zones are confined on both sides by a 200 nm Al<sub>0.35</sub>Ga<sub>0.65</sub>As<sub>0.03</sub>Sb<sub>0.97</sub>/20 nm-AlSb sequence.

*In situ* reflection high-energy electron diffraction (RHEED) was used to monitor the growth mode. As grown samples have been characterized by high-resolution x-ray diffraction (HRXRD) coupled to pattern simulations using the X'PERT EPITAXY™ software, transmission electron microscopy (TEM), and photoluminescence (PL) spectroscopy. Cross-sectional TEM specimens were prepared by using mechanical thinning followed by Ar-ion milling. The TEM investigations were performed in a JEOL JEM 3010 microscope operating at 300 kV. PL was excited with a 780 nm GaAs diode laser, analyzed by a Fourier transform IR spectrometer and detected by a liquid-nitrogen cooled InSb photodetector.

We show in Fig. 1(a) the RHEED pattern observed along

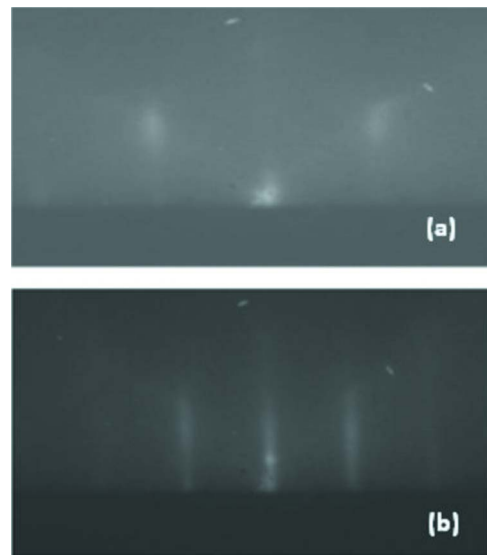


FIG. 1. (Color online) RHEED patterns taken along the  $[1\bar{1}0]$  azimuth after (a) completion of a 7 ML Ga<sub>0.50</sub>In<sub>0.50</sub>As layer and (b) growth of 2 ML GaSb atop the 7 ML Ga<sub>0.50</sub>In<sub>0.50</sub>As layer.

<sup>a)</sup>Electronic addresses: etournie@univ-montp2.fr and eric.tournie@univ-montp2.fr.

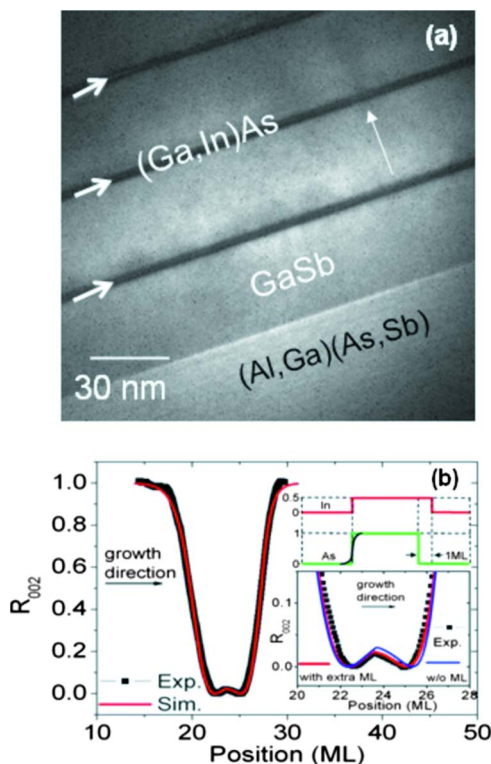


FIG. 2. (Color online) (a) (002)dark-field TEM micrograph taken from a 3 periods [30 nm GaSb/7 ML  $\text{Ga}_{0.5}\text{In}_{0.5}\text{As}$ ] heterostructure, (b) measured intensity ratio  $R$  across the interface and the corresponding simulations based on the In- and As-profiles given schematically in the upper inset (a representation of the sigmoidal function is shown for the As-profile). Lower inset: zoom on the simulations with/without the extra  $\text{Ga}_{0.5}\text{In}_{0.5}\text{Sb}$  ML compared to the experimental data.

the  $[1\bar{1}0]$  azimuth after completion of 7 ML  $\text{Ga}_{0.5}\text{In}_{0.5}\text{As}$  on GaSb at 420 °C. The tensile strain is then  $-3.9\%$ . Clear 3D spots are observed which reveal the formation of QDs according to the SK growth mode. RHEED observations indicate that all  $\text{Ga}_{1-x}\text{In}_x\text{As}$  alloys ( $0 \leq x \leq 0.50$ ) grow on GaSb in the SK mode, with a 2D–3D critical thickness which varies from  $\sim 1.7$  ML for GaAs to 4 ML for  $\text{Ga}_{0.5}\text{In}_{0.5}\text{As}$ . In all cases, the RHEED pattern returns to 2D-like characteristics again after the growth of  $\sim 2$  ML GaSb-barrier only [Fig. 1(b)].

We now show in Fig. 2(a) a dark-field TEM micrograph taken under the chemical sensitive (002) imaging conditions from the sample with nominal 7 ML  $\text{Ga}_{0.5}\text{In}_{0.5}\text{As}$  embedded in GaSb barriers, i.e., with a layer thickness well beyond the 2D–3D transition. While *in situ* RHEED observations confirm the 3D growth front, the TEM micrograph surprisingly does not reveal any 3D interface morphology. On the contrary, the  $\text{Ga}_{1-x}\text{In}_x\text{As}$  layer appears as structurally perfect 2D quantum well (QW) with smooth interfaces and a homogeneous composition within the QW. The interface profiles are analyzed from intensity area scans across the interfaces using the dedicated approach explained in detail in Refs. 4 and 5. This analysis is based on distribution profiles for the different constituent elements which are inserted into the calculation of the corresponding diffracted intensity under kinematic conditions ( $I_{002}$ ). The simulated intensity ratio  $R$  (equal to  $I_{002}/I_{002}^{\text{ref}}$  referred to the intensity of the barrier) is fitted to the experimental one by varying the composition profiles as shown in Fig. 2(b). The profiles are represented by the sig-

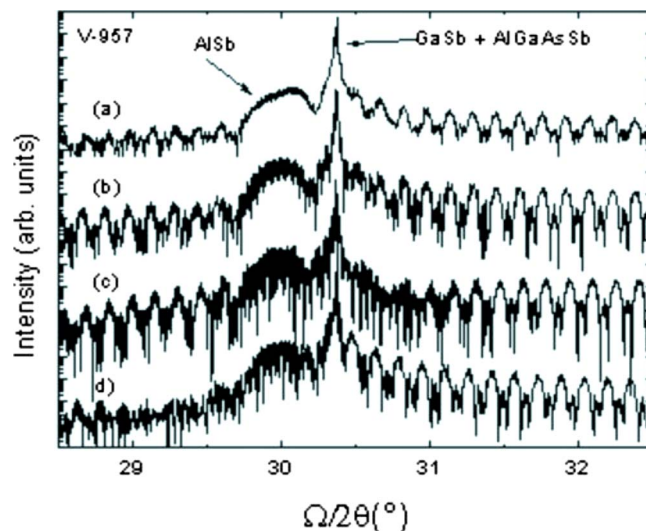


FIG. 3. (Color online) HRXRD patterns for a nominal 7 ML  $\text{Ga}_{0.5}\text{In}_{0.5}\text{As}/\text{GaSb}$  heterostructure: (a) experimental, (b) simulation considering that the upper ML has been transformed into 1 ML  $\text{Ga}_{0.5}\text{In}_{0.5}\text{Sb}$ , (c) simulation assuming the nominal QW, (d) simulation assuming that the last 2 MLs have been transformed into 2 ML  $\text{Ga}_{0.5}\text{In}_{0.5}\text{Sb}$ . The curves have been vertically shifted for the sake of clarity.

moidal functions with the interface width as main fitting parameter<sup>4,5</sup> and final concentration values inside the QW of 0.5 and 1 for In and As, respectively [cf. upper inset in Fig. 2(b)]. The best fit results in an In concentration distribution that is 1 ML wider than the As-profile, as it is demonstrated by the clear deviation of the simulation compared to the experimental curve when neglecting this “extra” ML [lower inset in Fig. 2(b)]. It is remarkable that the sensitivity of the simulation is higher than the resolution of the aperture dependent dark-field method. We therefore conclude that around 1 ML  $\text{Ga}_{0.5}\text{In}_{0.5}\text{As}$  has been converted in 1 ML  $\text{Ga}_{0.5}\text{In}_{0.5}\text{Sb}$  at the upper interface during overgrowth by GaSb. In turn, we show in Fig. 3 the experimental and simulated HRXRD patterns from the same sample. Simulations have been performed assuming perfect 2D QWs and 1 ML [Fig. 3(b)], 0 ML [Fig. 3(c)], or 2 ML [Fig. 3(d)]  $\text{Ga}_{0.5}\text{In}_{0.5}\text{Sb}$  inserted at the upper interface. Careful examination of the satellite positions and envelopes reveals that the best agreement between experiment [Fig. 3(a)] and simulation is achieved with a 1 ML  $\text{Ga}_{0.5}\text{In}_{0.5}\text{Sb}$  additional layer [Fig. 3(b)]. In contrast, noticeable discrepancies exist at high angles when assuming the nominal layer structure [Fig. 3(c)] or at low angles when assuming insertion of 2 ML  $\text{Ga}_{0.5}\text{In}_{0.5}\text{Sb}$  [Fig. 3(d)]. Thus, the x-ray simulations do confirm the presence of an additional 1 ML  $\text{Ga}_{0.5}\text{In}_{0.5}\text{Sb}$  but they cannot tell at which interface it is located. However, given the RHEED and TEM observations detailed above we suggest that it has to be located at the upper interface.

These observations are very surprising since *in situ* RHEED revealed a clear 2D–3D transition while *ex situ* observations do not show any hint for such a transition. This behavior differing from the well known  $\text{Ga}_{1-x}\text{In}_x\text{As}$  in GaAs case,<sup>2</sup> we ascribe it to the presence of Sb in our materials system. As shown above, RHEED indicated a very fast recovery toward a 2D morphology upon GaSb-growth initiation [cf. Fig. 1(b)]. Now, Sb has been shown to behave as a surfactant which delays or prevents the 2D–3D transition during the growth of strained  $\text{Ga}_{1-x}\text{In}_x\text{As}$  or  $\text{Ga}_{1-x}\text{In}_x\text{N}_y\text{As}_{1-y}$

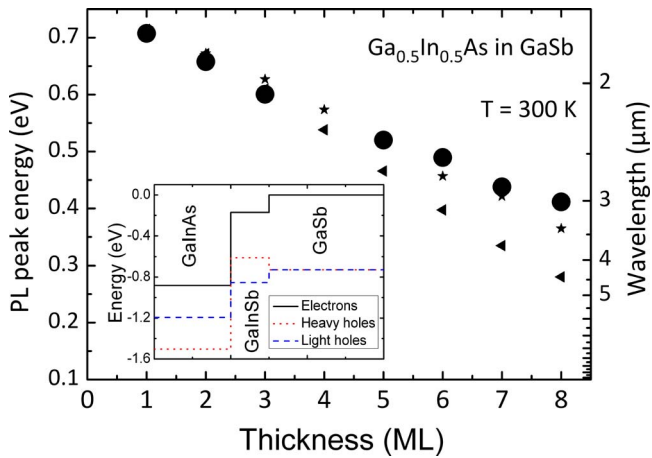


FIG. 4. (Color online) Experimental and calculated PL-peak energy for  $\text{Ga}_{0.5}\text{In}_{0.5}\text{As}/\text{GaSb}$  QWs: ● experimental data, ▲ calculation assuming nominal tensile-strained  $\text{Ga}_{0.5}\text{In}_{0.5}\text{As}$  QWs, and ★ calculation assuming 1 ML compressively strained  $\text{Ga}_{0.5}\text{In}_{0.5}\text{Sb}$  at the upper interface. The size of the experimental-data symbols corresponds to the error bar. The inset shows the band alignments used in the calculations with  $\text{Ga}_{0.5}\text{In}_{0.5}\text{As}$  and  $\text{Ga}_{0.5}\text{In}_{0.5}\text{Sb}$  considered under tension and compression, respectively. All energies are referred to the bulk GaSb conduction band.

layers on GaAs substrates.<sup>6,7</sup> In addition, in the tensile-strained  $\text{Ga}_{1-x}\text{In}_x\text{As}/\text{GaSb}$  heterostructure, the creation of a compressively-strained  $\text{Ga}_{1-x}\text{In}_x\text{Sb}$  layer at any interface decreases the overall strain, and thus stabilizes the system. The combination of these effects may explain the strong reorganization of the growth front observed at the upper interface which results in the observed QW microstructure.

Finally, we show in Fig. 4 the evolution with the QW width of the PL peak-position measured at 300 K for the  $\text{Ga}_{0.5}\text{In}_{0.5}\text{As}/\text{GaSb}$  samples. The emission enters deeply into the mid infrared range with a wavelength as long as 3.0  $\mu\text{m}$  for 8 ML  $\text{Ga}_{0.5}\text{In}_{0.5}\text{As}$ . Figure 4 also compares these experimental results to theoretical values calculated assuming either the nominal  $\text{Ga}_{0.5}\text{In}_{0.5}\text{As}/\text{GaSb}$  QW or the structure deduced from TEM, i.e., including 1 ML  $\text{Ga}_{0.5}\text{In}_{0.5}\text{Sb}$  at the upper QW interface. The PL peak energies have been calculated within the envelope-function ap-

proximation. Calculation was based on a transfer-matrix algorithm to describe our multilayered structures and used the bands alignment described in the inset of Fig. 4. It takes into account the strain state of the tensile- $\text{Ga}_{0.5}\text{In}_{0.5}\text{As}$  and compressive- $\text{Ga}_{0.5}\text{In}_{0.5}\text{Sb}$  layers, and the original band parameters compiled by Vurgaftman *et al.*<sup>8</sup> Experimental and calculated values of the PL-peak position rapidly diverge when assuming the nominal  $\text{Ga}_{0.5}\text{In}_{0.5}\text{As}$  QW while a very good agreement is obtained when inserting 1 ML  $\text{Ga}_{0.5}\text{In}_{0.5}\text{Sb}$  (Fig. 4). This again fits perfectly with the conclusions drawn from TEM observations.

In conclusion, we have studied the properties of highly-tensile strained  $\text{Ga}_{1-x}\text{In}_x\text{As}/\text{GaSb}$  nanostructures grown by MBE. We have demonstrated a peculiar behavior of this materials system where the  $\text{Ga}_{1-x}\text{In}_x\text{As}$  QDs spontaneously transform into QWs upon GaSb-growth initiation. We have shown that PL emission up to 3.0  $\mu\text{m}$  can be achieved at room temperature in good agreement with calculated values.

We acknowledge D. Steffen for her help with TEM specimen preparation. This work was partially funded by the French National Research Agency (ANR) in the frame of its program in Nanosciences and Nanotechnologies (MIR-NANO Project No. ANR-08-NANO-053).

<sup>1</sup>E. Bauer and H. Poppa, *Thin Solid Films* **12**, 167 (1972).

<sup>2</sup>*Semiconductor Quantum Dots*, edited by Y. Masumoto and A. Takagahara (Springer, Berlin, Heidelberg, 2002).

<sup>3</sup>N. N. Ledentsov, J. Böhrer, M. Beer, F. Heinrichsdorff, M. Grundmann, D. Bimberg, S. V. Ivanov, B. Ya. Meltser, S. V. Shaposhnikov, I. N. Yassievich, N. N. Faleev, P. S. Kop'ev, and Zh. I. Alferov, *Phys. Rev. B* **52**, 14058 (1995).

<sup>4</sup>E. Luna, F. Ishikawa, B. Satpati, J. B. Rodriguez, E. Tournié, and A. Trampert, *J. Cryst. Growth* **311**, 1739 (2009).

<sup>5</sup>E. Luna, B. Satpati, J. B. Rodriguez, A. N. Baranov, E. Tournié, and A. Trampert, *Appl. Phys. Lett.* **96**, 021904 (2010).

<sup>6</sup>D. S. Jiang, Y.-H. Qu, H.-Q. Ni, D.-H. Wu, Y.-Q. Xu, and Z.-C. Niu, *J. Cryst. Growth* **288**, 12 (2006).

<sup>7</sup>X. Yang, M. J. Jurkovic, J. B. Heroux, and W. I. Wang, *Appl. Phys. Lett.* **75**, 178 (1999).

<sup>8</sup>I. Vurgaftman, J. R. Meyer, and L. R. Ram-Mohan, *J. Appl. Phys.* **89**, 5815 (2001).